

## Original papers

# Association of hemophagocytic lymphohistiocytosis with kidney lesions in acute African swine fever virus infection

Naira Yu. Karalyan<sup>1</sup>, Marina R. Tatoyan<sup>2</sup>, Anna B. Semerjyan<sup>3</sup>,  
Narek H. Nersisyan<sup>4</sup>, Zara B. Semerjyan<sup>4</sup>, Lina H. Hakobyan<sup>4</sup>,  
Zaven A. Karalyan<sup>3,4,5</sup>

<sup>1</sup>Department of Pathological Anatomy and Clinical Morphology, Armenia Yerevan State Medical University, 2 Koryun St., Yerevan 0025, Armenia

<sup>2</sup>Department of Cytology, Histology and Embryology, Armenia Yerevan State Medical University, 2 Koryun St., Yerevan 0025, Armenia

<sup>3</sup>Department of Medical Biology and Parasitology, Armenia Yerevan State Medical University, 2 Koryun St., Yerevan 0025, Armenia

<sup>4</sup>Laboratory of Cell Biology and Virology, Institute of Molecular Biology of NAS RA, 7 Hasratyan St., Yerevan 0014, Armenia

<sup>5</sup>Department of Bioengineering, Bioinformatics and Molecular Biology, Russian-Armenian (Slavonic) University, 123 Hovsep Emin St., Yerevan 0051, Armenia

Corresponding Author: Zaven A. Karalyan; e-mail: zkaralyan@yahoo.com

**ABSTRACT.** Glomerulonephritis due to African swine fever (ASF) is well documented. However, there is absence of good understanding of mechanisms involved in the development of pathology development. This study examines glomerulonephritis in association with acute infection induced by II genotype (Georgia 2007) of ASF virus. Taken together, the results of urinary analysis and the renal histological analysis led to the diagnosis of diffuse endocapillary proliferative glomerulonephritis with severe tubular injury associated with acute ASF (Georgia 2007). According to the pathogenesis, we have found that the diffuse endocapillary proliferative glomerulonephritis associated with the acute ASF develops with a delay of one to two days compared to development of hemophagocytic lymphohistiocytosis. The diagnosis of endocapillary proliferative glomerulonephritis confirms the characteristic of pathological changes in the composition of urine and urine sediment. The development of acute proliferative glomerulonephritis begins at 3 dpi, and finished at 4–6 dpi with the development of tubular necrosis. Our study demonstrates local macrophage proliferation. Local proliferation may be an important mechanism for amplifying macrophage-mediated renal injury. We have shown that the development of diffuse acute proliferative glomerulonephritis during ASF does not coincide with the presence of the virus in the blood or kidney tissues, but coincides with the developmental of ASFV derived hemophagocytic lymphohistiocytosis. The development of hemophagocytic lymphohistiocytosis also begins at least at 2–3 dpi and continues up to the terminal stage of the disease.

**Key words:** African swine fever, diffuse endocapillary proliferative glomerulonephritis, hemophagocytic lymphohistiocytosis, proteinuria, haemolysis

## Introduction

African swine fever virus (ASFV) has spread rapidly into Armenia, vast areas of western and southern Russia, and also Ukraine and Belarus since its introduction into Georgia [1]. In 2014 ASF entered into Lithuania, Poland, Latvia, and Estonia;

in 2017 first time reported in Czech Republic and Romania, and in 2018 summer an outbreak of ASF has been reported in China [2,3]. African swine fever (ASF) is a highly lethal disease of domestic pigs caused by the only known DNA arbovirus. In pigs, ASFV replicates in the cells of the mononuclear phagocyte system, predominantly in

monocytes and macrophages. Several other cell types can be infected, especially in the later stages of the disease. Many scientists consider that the massive destruction of macrophages plays a major role in pathogenesis, especially in the impaired haemostasis due to the release of active substances like cytokines, complement factors etc. But despite intensive research efforts, most of these pathogenetical aspects are still far from being understood [4].

The screening of the tests on clinically healthy animals to diagnose a disease and to assess its severity and consequences, the formulation of a prognosis and the monitoring of the response of therapy or the progression of the disease are the reasons that the hematological and biochemical profiles are commonly performed in veterinarian medicine. Despite of their clinical importance, their interpretation are sometimes difficult as many factors can significantly modify the laboratorial parameters, such as gender, age, breed, diet, environmental conditions, samples management, laboratorial procedures, health status and subclinical diseases [5].

The renal involvement in acute ASF is one of the significant factors in determining severity of disease. There are several reports about development of diffuse acute proliferative glomerulonephritis during ASF [6]. The histopathology which is describing glomerular hypercellularity, acute diffuse proliferative glomerulonephritis, and glomerular necrosis has been shown previously [7]. However, there is absence of good understanding of mechanisms involved in the pathology of development. Our previous investigations have been shown that the hemophagocytic lymphohistiocytosis is an important part of the pathogenesis of ASF [8]. According to the modern understanding the renal lesions of HPs are polymorphic and can affect almost every structure of the kidney [9].

The aim of the present study is to describe gross, histopathologic lesions, pathological changes occur in clinical biochemistry of serum and urine as well as urine sediment analyst in pigs with acute ASF and its comparison in timing and sequence of appearance with the development of hemophagocytic lymphohistiocytosis.

## Materials and Methods

**Virus.** Infections were carried out using ASFV (genotype II) distributed in Republic of Armenia and Republic of Georgia [10]. The titer of ASFV for each intramuscular injection was  $10^4$  hemadsorbing doses

(HAD<sub>50</sub>)/ml. Virus titration was done as described previously and expressed as  $\log_{10}$  HAD<sub>50</sub>/ml [11].

**Animals.** In our study, seventeen pigs (n=17) (Landrace breed) of the same age (3-month-old) and weight (30–33 kg) were used for infection and three for control. Infected pigs were euthanatized in batches of three at 2, 3, 4, and of 4 at 6 and 7 days post-infection (dpi). Three control pigs were euthanatized at the end of the experiment.

Animal care and euthanasia were done according to the AVMA Guidelines on Euthanasia, and local guideline for animal care and use (Institutional Review Board/Independent Ethics Committee of the Institute of Molecular Biology of NAS, IRB00004079). Carbon dioxide inhalation (75–80% carbon dioxide for 20–60 min) was used to euthanize infected and control animals after 7 days post infection (dpi).

**Tissue samples.** Samples from kidneys were fixed in 10% buffered formalin solution (pH 7.2) for 24 hours. After fixation, the samples were dehydrated through a graded series of alcohols, washed with xylol and embedded in paraffin wax by a routine technique for light microscopy. For structural analysis, wax-embedded samples were cut (Microm HM 355, 5  $\mu$ m) and stained with hematoxylin and eosin in accordance with the manufacturer's protocol (Sigma-Aldrich, Germany). The histological examination was performed using a light microscope.

**Serum biochemistry.** Serum chemical determinations were done with a COBAS Integra 400 analyzer. Authentic reagents (Roche) were used in the determination of all blood indices.

**Urine chemistry.** Urine chemistry was evaluated using Test Strips from Roche Diagnostics (on Urisys-1100 analyzer) and freshly expressed urine.

**Urine cytology.** Fresh urine samples were collected and processed immediately. The aliquots of 15 mL of urine were centrifuged for 10 minutes at 1,500 rpm. The supernatant was discarded, and the cell pellet was resuspended in a small volume of urine. Centrifugation of the resuspended aliquots was used to prepare 4 ethanol (95%) and 1 air-dried smear. A minimum of 20 high-power fields (HPF) were examined, and a differential count of the various cellular elements was done on the May-Grünwald-Giemsa-stained smears. Epithelial cells from the lower urinary tract and urothelial cells also were counted.

**Statistical analysis.** Statistical analyses were performed using the Student's t-test and Mann-

Whitney u-test. SPSS version 17.0 software package (SPSS Inc., Chicago, Illinois) was used for statistical analyses

## Results

### Experimental infection

Acute form of the ASF was described on Malawi' 83 ASFV isolate. The clinical signs of experimental infection have some differences in comparison with those which have been cited in the research of Malawi' 83 ASFV isolate [7,12].

The first clinical signs were observed at 2–3 dpi when all infected pigs demonstrated loss of appetite and depression. From 2 to 4 dpi, infected animals displayed hyperthermia with body temperature more than 40°C. Simultaneously, decreased activity in behavior, difficulties in breathing and reddening of the skin were detected. Melena (present only in 2 animals from 9–22% cases) and lethargy were seen at 5–7 dpi, and therefore all infected animals were sacrificed according to guidelines at 7th dpi. Although infected animals were asymptomatic up to 3 dpi, viremia appeared from 1–2 dpi and peaked on 5–6 dpi (viremia titers were 5.0–5.75 log<sub>10</sub> HAD<sub>50</sub>/ml). The high titers of ASFV were determined in all pigs up to 7th dpi (Fig. 1).

ASF experimental infection was characterized by early viremia from 1–2 dpi. Viremia peaked on 5th dpi (virus titres were 5.0–5.25 log<sub>10</sub> HAD<sub>50</sub>/ml). The high titres of ASFV were determined in all pigs up to 7 dpi.

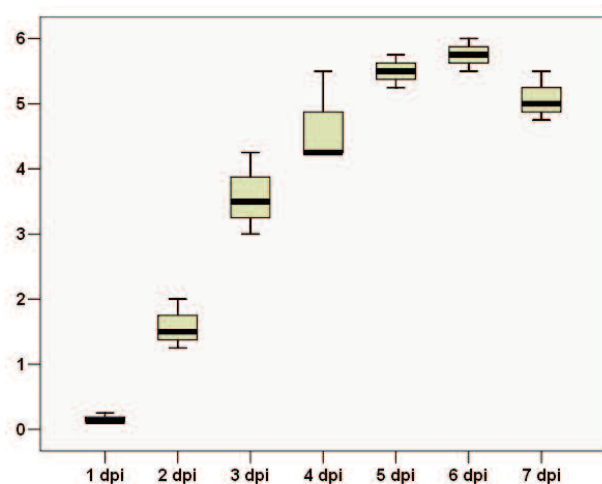


Fig. 1. ASFV titer during acute infection in swine. Virus yields at different times post-infection (X axis) are expressed as log<sub>10</sub> HAD<sub>50</sub>/ml (Y axis). Each point represents the mean of viral titer. Error bars indicate the standard errors.

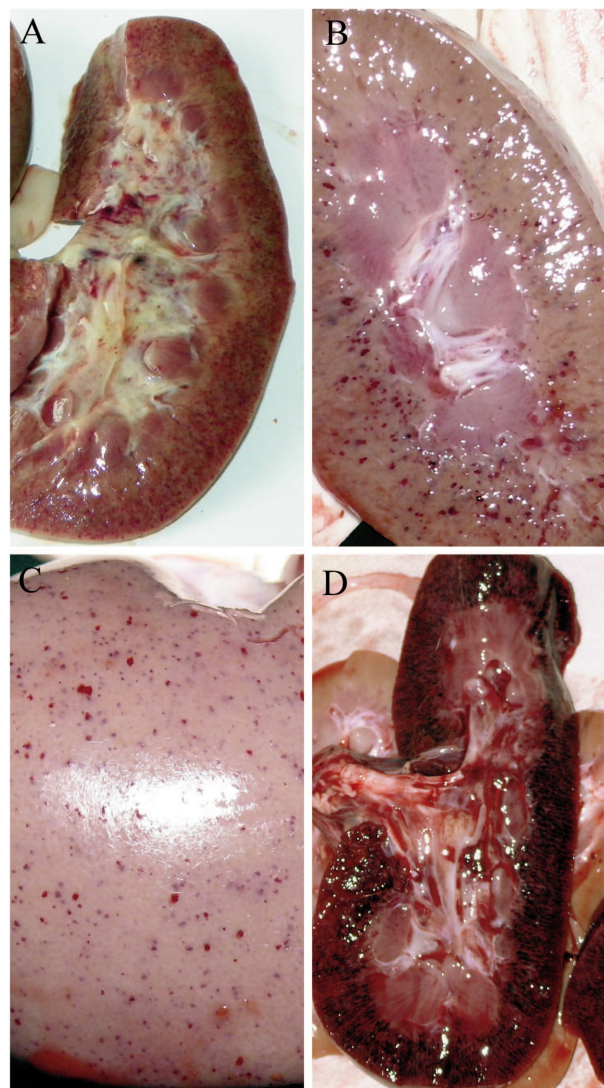


Fig. 2. Gross pathology of kidney at acute African swine fever. A. Subcapsular kidney haemorrhages at 3 dpi; B. Kidney haemorrhages at 4 dpi; C. Pig kidneys with multiple small hemorrhages at 6th dpi; D. Confluent haemorrhages in kidneys at 7th dpi.

### Gross necropsy of kidneys

All of investigated kidneys were normal in the controls and the infected pigs on 2nd dpi. Kidneys became enlarged, the sub-capsular surface of the kidney and the mucosa of the urinary bladder were petechiated after 3rd dpi (3 of 6 kidneys affected – 50%). At 4th dpi all pathological changes were the same, in some cases haemorrhages became bigger (Fig. 2A,B) (4 of 6 kidneys affected – 67%). At 6th dpi were affected majority of kidneys (6 of 8 – 75%). The same changes occurred at 6–7th dpi (6 of 8 kidneys affected – 75%), haemorrhages often became visible in intact kidney (Fig. 2C). Sometimes it was observed confluent haemorrhages

Table 1. Urine chemistry for pigs with ASF in disease dynamics

| Parameters       | control     | 1 dpi     | 2 dpi     | 3 dpi     | 4 dpi       | 5 dpi      | 6 dpi       |
|------------------|-------------|-----------|-----------|-----------|-------------|------------|-------------|
| Urobilinogen     | negative    | negative  | negative  | negative  | negative    | negative   | negative    |
| pH               | 5.5 ± 0.5   | 6.0 ± 0.5 | 6.0 ± 0.5 | 6.5 ± 0.5 | 6.5 ± 0.5   | 5.5 ± 0.5  | 5.4 ± 0.5   |
| Blood            | negative    | +         | +++*      | +++*      | +++*        | +++*       | +++*        |
| Bilirubin        | negative    | negative  | negative  | negative  | +           | +          | +           |
| Ketones          | negative    | negative  | negative  | negative  | negative    | negative   | negative    |
| Glucose          | negative    | negative  | negative  | negative  | negative    | negative   | negative    |
| Protein (mg/l)   | <150        | 152 ± 19  | 420 ± 45* | 354 ± 31* | 435 ± 54*   | 987 ± 109* | 5554 ± 603* |
| Specific gravity | 1017 ± 5    | 1016 ± 4  | 1016 ± 5  | 1018 ± 3  | 1017 ± 4    | 1019 ± 4   | 1020 ± 4    |
| Color            | pale yellow | yellow    | yellow    | yellow    | dark yellow | amber      | amber       |
| Turbidity        | clear       | clear     | clear     | clear     | clear       | clear      | low turbid  |

\*significant compared with control ( $p < 0.05$ - $p < 0.001$ ); \*\*number of inversions 2 ( $p < 0.1$ ).

in kidneys (1 of 8 kidneys – 12.5%). Kidney with confluent haemorrhages became bigger and dark-red coloured (Fig. 2D).

### Histopathology of kidneys

Renal tubule lesions first arise in the distal tubules, and are less intense in the collecting ducts. Like in previous articles [6] at the initial phases of the disease (beginning from the 3 dpi), the tubules show evidence of degeneration, with destruction of

the apical portion of the epithelial cells and the necrosis of the subsequent epithelial cell. From 3 dpi in the proximal and distal convoluted tubules of the nephron was observed the destroyed parts of cells (Fig. 3D). This roughly coincides with identification of the proteinuria (Table 1), as well as with hyaline and granular casts in urine (Table 2).

Glomeruli are diffusely large and in the cells it begins 3 dpi (Fig. 3G,J), also were detected proliferation of mesangial cells (Fig. 3H,I), as

Table 2. Urine sediment for pigs with ASF in disease dynamics in field of view

| Parameters                           | control | 1 dpi               | 2 dpi | 3 dpi | 4 dpi | 5 dpi | 6 dpi   |
|--------------------------------------|---------|---------------------|-------|-------|-------|-------|---------|
|                                      |         | Cellular structures |       |       |       |       |         |
| RBC                                  | –       | 0-2                 | 5-7   | 5-7   | 2-3   | 7-10  | 15-17*  |
| dysmorphic RBC                       | –       | –                   | –     | –     | –     | –     | –       |
| WBC                                  | 0-3     | 2-3                 | 3-5   | 3-5   | 15-16 | 9-10  | 7-8     |
| renal epithelial cell                | –       | –                   | –     | –     | –     | 0-2   | 2-3     |
| transitional epithelial cell         | –       | –                   | –     | –     | 0-2   | 1-3   | 1-3     |
| Pavement or squamous epithelial cell | 0-5     | –                   | 3-4   | 3-4   | 5-7   | 3-5   | 7-8     |
| Bacteria**                           | –       | –                   | +     | +     | +     | +     | +       |
|                                      |         | Casts               |       |       |       |       |         |
| hyaline cast                         | –       | –                   | 0-1   | 0-2   | 1-2   | 3-5   | 4-5     |
| granular cast                        | –       | –                   | 3-4   | 2-3   | 1-2   | 4-5   | 5-7     |
| RBC cast                             | –       | –                   | –     | –     | –     | –     | –       |
| WBC cast                             | –       | –                   | –     | –     | –     | –     | –       |
| waxy cast                            | –       | –                   | –     | –     | –     | –     | –       |
|                                      |         | Crystals            |       |       |       |       |         |
| Uric acid                            | –       | –                   | –     | –     | 0-1   | 1-3   | 1-3     |
| Amorphous phosphates                 | –       | –                   | –     | –     | –     | –     | –       |
| Triple phosphate****                 | –       | –                   | –     | 0-3   | –     | –     | –       |
| Ca-oxalate monohydrate               | –       | –                   | –     | –     | –     | –     | –       |
| Amorphous urates                     | –       | –                   | –     | –     | 1-3   | 1-3   | 2-4**** |

\*excluded pig with macroscopic hematuria; \*\*bacteriuria was detected in two pigs (20%); \*\*\*number of inversions 2 ( $p < 0.1$ );

\*\*\*\*triple phosphates were detected in two pigs (20%).

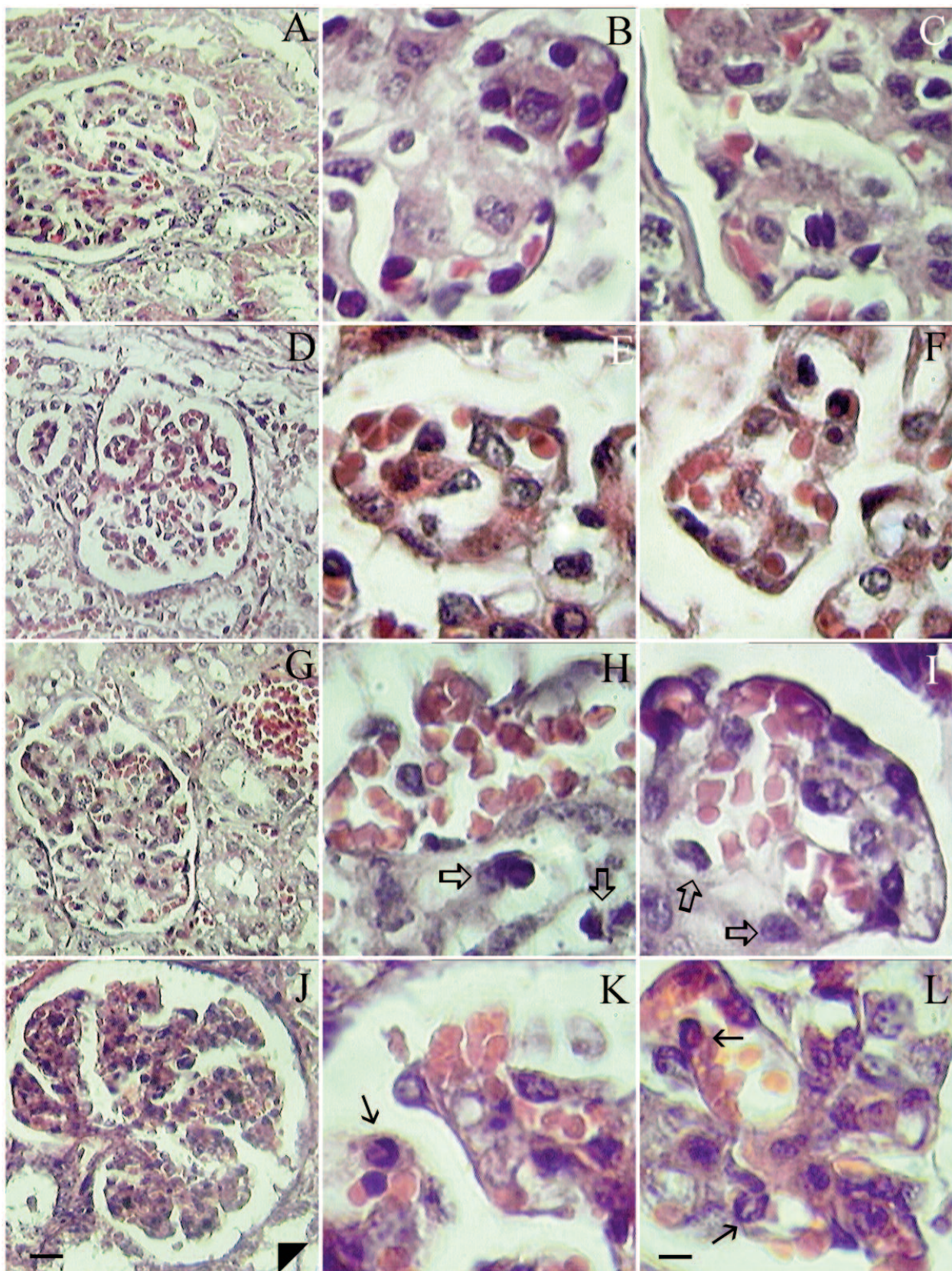


Fig. 3. Renal biopsy findings (light microscopy, HE staining)  
 1st row – control; 2nd row – 3 dpi; 3rd row – 4 dpi; 4th row – 6 dpi. Beginning 3 dpi glomeruli are diffusely large and cellular, at late stage of ASF – tubular necrosis (triangles) with the infiltration of neutrophils (black arrows) and proliferation of mesangial cells (transparent arrows). First column scale bar is 40  $\mu$ m. Second and third columns scale bar is 10  $\mu$ m.

Table 3. Compared dynamics of development of pathology in hemophagocytic lymphohistiocytosis and kidney

| Days  | Indices  |   |                                 |
|-------|--|---|---------------------------------|
|       | hemophagocytic lymphohistiocytosis                                 | renal pathology                           | viraemia HADU <sub>50</sub> /ml |
| 1 dpi | increased levels of MCSF   | –   | 0.125–0.25                      |
| 2 dpi | foamy macrophages  | hematuria, proteinuria,<br>granular casts | 1.25–2                          |
| 3 dpi | hemophagocytic and foamy macrophages,<br>increased levels of GMCSF | gross pathology,<br>histopathology        | 3–4.25                          |

compared to control (Fig. 3A,B,C).

At the 4–5 dpi erythrocytes were seen out of the vessels (Fig. 3K,L). And the late stages of ASF (5–6 dpi) led to considerably more profound histopathologic changes: appearance of local necrotic foci, single hemorrhages. No thickening or double contouring of capillary loop was seen (Fig. 3G,J).

The revealed glomerulonephritis is described as variant with proliferative characteristics of the diffuse endocapillary. In favor of this, an increase in glomeruli size, hypercellularity (Fig. 3E,F), pronounced proliferation of endothelial cells with an increase in the number of neutrophils (Fig. 3K,L).

### Biochemical profile

A biochemical profile which included glucose, urea nitrogen, creatine kinase, creatinine, GGT, cholesterol, sodium, potassium, calcium and phosphorus was done on eleven pigs (5–7 dpi). There were no significant differences in these parameters between infected and control pigs.

### Urine chemistry

Changes which were observed in the urine chemistry of pigs infected with ASFV are summarized in Table 2. Urine chemistry was done on 14 pigs (from 4th to 7th dpi) with ASF and was compared to controls (Table 1). Urine from pigs with ASF was generally clear and deep yellow up to amber in color.

As follows from the Table 1, during ASF development were observed presence of blood in urine, bilirubinuria, proteinuria, changes in urine color. Macroscopic hematuria was found in only one pig (10%) at the terminal stage of disease.

### Urine sediment analyses

Eleven pigs (5–7 dpi) with acute ASF were tested on urine sediment and the results summarized in Table 2.

As follows from Table 2, ASFV infection caused an increase in the number of white blood (leukocytes) and squamous epithelial cells, arising

of RBC, renal and transitional epithelial cells as well as hyaline and granular casts in urine sediment.

Crystalluria was investigated in ten ASFV infected pigs, the same pigs were used as controls before virus injection. Two pigs were used as healthy controls in experiment.

Investigations of crystalluria in urine detected that ASFV infection caused arising uric acid and amorphous urates crystals. Triple phosphate crystals were detected in 2 pigs with bacteriuria.

### Comparison of development of dynamics in renal pathology and hemophagocytic lymphohistiocytosis

The Table 3 shows the timelines of the emergence of key development indicators for renal pathology and hemophagocytic lymphohistiocytosis, used data Karalyan et al. [8], aroused at acute ASF.

The comparison of the two pathological processes shows that the hemophagocytic lymphohistiocytosis precedes or develops simultaneously with renal pathology.

### Discussion

In human acute kidney injury is the most common kidney pathology manifestation of hemophagocytic lymphohistiocytosis and is generally considered a poor prognostic factor. The most common histologically observed pathology is acute tubular necrosis. Rarely, renal pathology with hemophagocytic lymphohistiocytosis associated with severe interstitial inflammatory infiltrates of lymphocytes and activated macrophages, and intrarenal hemophagocytosis has been described by infiltrating interstitial macrophages [13,14].

Our data suggest pathophysiological mechanism that may be responsible for the impairment of renal function during ASF derived hemophagocytic lymphohistiocytosis: acute tubular necrosis and/or reduction of the glomerular filtration flow resulting

from the massive collapses of glomerular tufts.

We have shown that the development of diffuse acute proliferative glomerulonephritis during ASF does not coincide with the presence of the virus in the blood or kidney tissues [15], but coincides with the developmental of ASFV derived hemophagocytic lymphohistiocytosis. The development of hemophagocytic lymphocytosis also begins at least at 2–3 dpi and continues up to the terminal stage of the disease [8]. Urinalysis revealed mild proteinuria at 2 dpi and severe proteinuria at terminal stage of disease. Persistent and increased protein levels in the urine are abnormal. Renal loss of plasma proteins can contribute to several pathologies including hypoalbuminemia; alterations in coagulation factors, cellular immunity, hormonal status etc. But all they are a sign of renal damage. Proteinuria, especially at late stages of the disease reflects a severe glomerulonephritis. This, in combination with other urine sediment findings such as hematuria and hyaline casts reinforce this diagnosis. Glomerulonephritis does not often diagnosed in swine but has been reported as a sequel to some viral diseases such as hog cholera, African swine fever [6].

This study shows that haematuria is commonly associated with acute ASF. Occasionally it can cause macroscopic haematuria (10%). Some of the causes of haematuria are because of urinary origin, and include glomerulonephritis, infectious nephrolithiasis, neoplasia, cystic disease, infarction, trauma, parasites, and strenuous exercise; others are idiopathic. Extraordinary causes may include disorders of bleeding and coagulation, or disorders of the reproductive tract.

Examination of the urine sediment (Table 2) observed the presence of granular casts and renal epithelial cell casts at the late stage of disease. Usually this is consistent with the diagnosis of acute tubular necrosis [16]. The presence of erythrocytes in urine sediment, in association with proteinuria is assumed to be evidence for glomerular damage [17]. Granular casts and renal epithelial cells in sediment could be signs of acute tubular necrosis at late stages of the disease. Uric acid crystals are most probably the results of massive cellular destruction that has been described in this disease [18].

Crystalluria (Table 2) refers to crystals found in the urine and can be associated with pathological conditions such as urolithiasis, acute uric acid nephropathy etc. Sometimes small amounts of crystals can occur in animals with normal urinary

tracts without any clinical signs of lower urinary tract disease, so their detection usually has auxiliary information.

Amounts of uric acid crystals or “amorphous material” may be found in the urine of patients with aggressive lymphoproliferative disorders [19]. Thus, their presence indirectly indicates the important role of hyperactivation of immune system in the development of glomerulonephritis.

Triple phosphate crystals (detected in 20% cases) are typical for infected urine, especially that caused by urea-splitting bacteria (Fogazzi, 1996), and they are detected in pigs with bacteriuria.

Thus, pathohistological studies have revealed diffuse endocapillary proliferative glomerulonephritis, developing under the influence of ASFV (Georgia 2007). The diagnosis of endocapillary proliferative glomerulonephritis confirms the characteristic pathological changes in the composition of urine and urine sediment. The development of acute proliferative glomerulonephritis begins at 3 dpi, and finished at 4–6 dpi with the development of tubular necrosis.

## Acknowledgements

This work was supported by a grant from the Russian-Armenian (Slavonic) University at the expense of the Ministry of Education and Science of the Russian Federation.

## Conflicts of interest

The sponsors had no input into study design, collection, analysis or interpretation of the data or in the decision on where to submit the manuscript.

## References

- [1] Oura C. 2013. African swine fever virus: on the move and dangerous. *Veterinary Record* 173: 243-245. doi:10.1136/vr.f5327
- [2] Jurado C., Martínez-Avilés M., De La Torre A., Štukelj M., de Carvalho Ferreira H.C., Cerioli M., Sánchez-Vizcaíno J.M., Bellini S. 2018. Relevant measures to prevent the spread of African swine fever in the European Union domestic pig sector. *Frontiers in Veterinary Science* 5: 77. doi:10.3389/fvets.2018.00077
- [3] Li X., Tian K. 2018. African swine fever in China. *Veterinary Record* 183: 300-301. doi:10.1136/vr.k3774
- [4] Blome S., Gabriel C., Beer M. 2013. Pathogenesis of

- African swine fever in domestic pigs and European wild boar. *Virus Research* 173: 122-130. doi:10.1016/j.virusres.2012.10.026
- [5] Muñoz A., Riber C., Trigo P., Castejón F. 2012. Age- and gender-related variations in hematology, clinical biochemistry, and hormones in Spanish fillies and colts. *Research in Veterinary Science* 93: 943-949. doi:10.1016/j.rvsc.2011.11.009
- [6] Hervás J., Gómez-Villamandos J., Méndez A., Carrasco L., Sierra M.A. 1996. The lesional changes and pathogenesis in the kidney in African swine fever. *Veterinary Research Communications* 20: 285-299. doi:10.1007/bf00366926
- [7] Gómez-Villamandos J.C., Hervás J., Méndez A., Carrasco L., Villeda C.J., Wilkinson P.J., Sierra M.A. 1995. Ultrastructural study of the renal tubular system in acute experimental African swine fever: virus replication in glomerular mesangial cells and in the collecting ducts. *Archives of Virology* 140: 581-589. doi:10.1007/bf01718433
- [8] Karalyan Z.R., Ter-Pogossyan Z.R., Karalyan N.Yu., Semerjyan Z.B., Tatoyan M.R., Karapetyan S.A., Karalova E.M. 2017. Hemophagocytic lymphohistiocytosis in acute African swine fever clinic. *Veterinary Immunology and Immunopathology* 187: 64-68. doi:10.1016/j.vetimm.2017.03.008
- [9] Karras A. 2009. What nephrologists need to know about hemophagocytic syndrome. *Nature Reviews Nephrology* 5: 329-336. doi:10.1038/nrneph.2009.73
- [10] Rowlands R.J., Michaud V., Heath L., Hutchings G., Oura C., Vosloo W., Dwarka R., Onashvili T., Albina E., Dixon L.K. 2008. African swine fever virus isolate, Georgia, 2007. *Emerging Infectious Diseases* 14: 1870-1874. doi:10.3201/eid1412.080591
- [11] Enjuanes L., Carrascosa A.L., Moreno M.A., Viñuela E. 1976. Titration of African swine fever (ASF) virus. *Journal of General Virology* 32: 471-477. doi:10.1099/0022-1317-32-3-471
- [12] Gómez-Villamandos J.C., Bautista M.J., Carrasco L., Caballero M.J., Hervás J., Villeda C.J., Wilkinson P.J., Sierra M.A. 1997. African swine fever virus infection of bone marrow: lesions and pathogenesis. *Veterinary Pathology* 34: 97-107.
- [13] Santoriello D., Hogan J., D'Agati V.D. 2016. Hemophagocytic syndrome with histiocytic glomerulopathy and intraglomerular hemophagocytosis. *American Journal of Kidney Diseases* 67: 978-983. doi:10.1053/j.ajkd.2015.11.017
- [14] Thauinat O., Delahousse M., Fakhouri F., Martinez F., Stephan J.-L., Noël L.-H., Karras A. 2006. Nephrotic syndrome associated with hemophagocytic syndrome. *Kidney International* 69: 1892-1898. doi:10.1038/sj.ki.5000352
- [15] Sierra M.A., Quezada M., Fernandez A., Carrasco L., Gomez-Villamandos J.C., Martin De Las Mulas J., Sanchez-Vizcaino J.M. 1989. Experimental African swine fever: evidence of the virus in interstitial tissues of the kidney. *Veterinary Pathology* 26: 173-176.
- [16] Chawla L.S., Domm A., Berger A., Shih S., Patel S.S. 2008. Urinary sediment cast scoring index for acute kidney injury: a pilot study. *Nephron Clinical Practice* 110: 145-150. doi:10.1159/000166605
- [17] Pillsworth T.J., Haver V.M., Abrass C.K., Delancy C.J. 1987. Differentiation of renal from non-renal hematuria by microscopic examination of erythrocytes in urine. *Clinical Chemistry* 33: 1791-1795.
- [18] Perazella M.A., Coca S.G., Hall I.E., Iyanam U., Korashy M., Parikh C.R. 2010. Urine microscopy is associated with severity and worsening of acute kidney injury in hospitalized patients. *Clinical Journal of the American Society of Nephrology* 5: 402-408. doi:10.2215/cjn.06960909
- [19] Fogazzi G.B. 1996. Crystaluria: A neglected aspect of urinary sediment analysis. *Nephrology Dialysis Transplantation* 11: 379-387. doi:10.1093/ndt/11.2.379

Received 18 February 2018

Accepted 17 October 2018